# *A Listeria monocytogenes aptasensor on laser inscribed graphene for food safety monitoring in hydroponic water*



**Citation:** Cavallaro, N., Moreira, G., Vanegas, D. et al. A Listeria monocytogenes aptasensor on laser inscribed graphene for food safety monitoring in hydroponic water. Discov Food 4, 169 (2024).

**As Published:** https://doi.org/10.1007/s44187-024-00251-z

**Publisher:** Springer International Publishing

**Persistent URL:** https://hdl.handle.net/1721.1/157839

**Version:** Final published version: final published article, as it appeared in a journal, conference proceedings, or other formally published context

**Discover** Food

Research

# A *Listeria monocytogenes* aptasensor on laser inscribed graphene for food safety monitoring in hydroponic water

**Nicholas Cavallaro[1] · Geisianny Moreira[2] · Diana Vanegas[3] · Dong Xiang[4] · Shoumen P. A. Datta[5,6] · Carmen Gomes[7] · Eric S. McLamore[2,3]**

Received: 2 March 2024 / Accepted: 25 November 2024
Published online: 03 December 2024


## Abstract

Consumption of fresh produce, such as leafy greens, is often encouraged as part of a healthy diet. Hence, indoor facilities for hydroponic production of leafy greens are increasingly being established. However, fresh produce entails a higher risk of microbial foodborne illnesses than processed foods. *Listeria monocytogenes* is a major source of fresh produce contamination and is among the leading causes of severe foodborne illnesses in the United States, with a 16% mortality rate. Tools for rapid monitoring are needed for pathogens such as *L. monocytogenes* to prevent outbreaks. In this manuscript, we have demonstrated the feasibility of a multi-aptamer approach for development of label-free aptasensors targeting *L. monocytogenes* in irrigation water for lettuce hydroponic production. We use screening studies with surface plasmon resonance to rationally develop mixtures of relevant aptamers for targeting *L. monocytogenes*. Based on this screening, multiple aptamers targeting extracellular structures on intact *L. monocytogenes* were tethered to platinum-modified laser inscribed graphene electrodes. This is the first report of a *L. monocytogenes* biosensor based on laser inscribed graphene. We show that mixing multiple aptamers with varying affinity improves the diagnostic performance over one aptamer alone in complex sample matrices (lettuce hydroponic water). Multi-aptamer biosensors showed high accuracy for *L. monocytogenes* and were at least three times more selective than *Escherichia coli* (Crooks, K12, O157:H7) with an accuracy of 85%. The limit of detection (10 CFU/10 mL) is based on data which were significantly different after calibration toward *L. monocytogenes* or *E. coli* (Crooks) and validated against gold standard molecular analysis (polymerase chain reaction). Rapid screening of pathogens is a global need to meet food safety and water quality regulations. This study shows the importance of sensors targeting more than one bacterial surface structure in complex samples relevant to the food-water nexus.

**Keywords** Listeria · Aptamer · Laser inscribed graphene · Biosensor · Lettuce · Foodborne pathogen

**Supplementary Information** The online version contains supplementary material available at https://doi.org/10.1007/s44187-024-00251-z.

✉ Eric S. McLamore, emclamo@clemson.edu | [1]Agricultural and Biological Engineering, Institute of Food and Agricultural Sciences, University of Florida, Gainesville, USA. [2]Agricultural Sciences, Clemson University, Clemson, USA. [3]Environmental Engineering and Earth Sciences, Clemson University, Clemson, USA. [4]School of Chemistry, Chemical Engineering and Biotechnology, Nanyang Technological University, Singapore, Singapore. [5]Department of Mechanical Engineering, MIT Auto-ID Labs, Massachusetts Institute of Technology, Cambridge, USA. [6]Biomedical Engineering Program, Department of Anesthesiology, MDPnP Labs, Massachusetts General Hospital, Harvard Medical School, Boston, USA. [7]Department of Mechanical Engineering, Iowa State University, Ames, USA.

## 1 Introduction

Among the United Nations' sustainable development goals (SDG), at least three are within the intersection of human health and the food supply chain. Two important aspects of the food system are access to nutritious products and food safety. Rapid global urbanization induces supply chain challenges for traditional food production systems, thus the urban food system must play an important role if we are to remain within planetary boundaries [1, 2]. Recent improvements in urban agriculture systems are fueled by developments in controlled environment agriculture (CEA) [3, 4]. Within CEA techniques, soil-less systems (i.e., hydroponic systems) will likely play a key role in future sustainable agricultural systems [5].

Large volumes of water are required for hydroponic systems [6]. Considering the ongoing need to reduce environmental pressures associated with industrial agriculture (including freshwater withdrawals, agrochemical pollution, and land occupancy), there is growing interest in implementing more sustainable strategies such as irrigating crops with alternative water sources (e.g., partially treated wastewater, and brackish water), implementing soilless cultivation systems amenable to urban food production (e.g. hydroponics, aquaponics, aeroponics), and more recently, integrating both wastewater recycling and soilless cultivation in closed-loop systems. Use of alternative water sources (AWS) for irrigation [7–9] poses unique safety risks to food consumers. Reuse of alternative water sources (AWS) is governed by local policy, and geography also plays a pivotal role in system efficiency [10]. One of the biggest challenges related to hydroponic food production systems are foodborne disease (FBD), which are communicable disease that pose risk to children, the elderly, and individuals with compromised immune systems [11]. FBD have been attributed to cause approximately 600 million illnesses and 420,000 deaths in one year which is likely an under-estimate [12]. The global burden is equivalent to 33 million disability adjusted life years (DALYS) [13].

Pathogenic *Listeria* are a major burden on public health systems [14]. One particular species, *L. monocytogenes*, is a leading cause of death associated with foodborne illness. *L. monocytogenes* accounts for a small fraction (< 0.05%) of the total cases of bacterial FBD in humans each year, but causes an annual economic burden of more than three billion dollars in the U.S. alone [15]. Outbreaks of foodborne pathogens such as *L. monocytogenes* can threaten food safety by increasing hospitalizations and deaths, thus leading to productivity losses in the food chain. Historically, *Listeria* contamination have occurred most commonly in products ranging from milk and dairy products [16] to cooked meat [17], smoked fish [18], and fresh produce [19, 20], among others. *L. monocytogenes* has shown the ability of developing antibiotic resistance [21] and is even able to adapt to the microenvironment within the gastrointestinal tract during chronic infection [22, 23].

In 2017, a single food product (processed meat) was responsible for an outbreak of listeriosis [24], impacting human health, the food industry, and national economy in South Africa. Short-term costs associated with this outbreak of *L. monocytogenes* were estimated to be $10.4 million in hospitalization costs, more than $240 million associated with loss of life, and more than $15 million in economic losses [25]. *L. monocytogenes*, among other pathogens, has been shown to persist in the most common type of hydroponic system used for lettuce production [26]. *L. monocytogenes* is known to persist on some fresh produce and microgreen tissues [19, 27], in lettuce leaf extract [28], across produce packing houses [29], and in hydroponic nutrient solution tanks [30]. The cultivation matrix/approach has been shown to impact the survivability of *L. monocytogenes* in hydroponic systems [31], and some studies have shown that the persistence of *L. monocytogenes* is greatly reduced (relative to soil systems) [32]. Although few outbreaks, if any, are directly linked to soil-less cultivation the risk of contamination of fresh produce is high. As hydroponic cultivation of produce increases, technologies such as rapid test kits may become even more relevant due to the transformation of agricultural practices toward urban production systems. Efforts to enhance surveillance of food products via development of alternative and affordable detection technologies are needed to achieve the public health outcomes proposed in the SDG. Rapid point-of-use-sensors, particularly sensors with embedded decision support, are one of the emerging tools which aim to provide rapid testing of food products [33–36].

The gold standard for *L. monocytogenes* monitoring and source tracking is whole genome sequencing (WGS) [37], which analyzes the entire set of genes in the *Listeria* genome. In the scenario of *Listeria* outbreaks, WGS is a powerful technique that allows tracking and comparison between *Listeria* isolates, linking *Listeria* to a contaminated source, and providing reliable data to support decision-making during an outbreak [38]. However, access to sequencing technologies or reliable networks for outsourcing analysis is a major challenge in most countries. Beyond WGS, molecular tests such as polymerase chain reaction (PCR) and enzyme-linked fluorescent assay (ELISA) are often used as an alternative diagnostic method for *Listeria* [39]. Despite standard centralized analysis (e.g., WGS, PCR, ELISA)

providing reliable results, these technologies require trained personnel to operate specific instruments and/or conduct sophisticated workflow protocols, which increases the associated cost for implementation and may make it unfeasible to deploy as a diagnostic tool, especially in economically challenged areas. To meet the diagnostic need, many technologies, such as biosensors, are emerging to provide on-site diagnostics with rapid screening capability. Label-free biosensors are one subclass of these emerging technologies for improving monitoring programs in the food supply chain [40–43].

Among the various techniques used to fabricate biosensors for foodborne pathogens, electrochemical devices are one of the most common (see reviews [44, 45]). Laser inscribed graphene (LIG) is one of the electrochemical sensor materials that is currently a leading candidate for low-cost, scalable fabrication of quantitative pathogen sensing devices [46, 47]. LIG biosensors have been created for detection of small molecules [48–51], proteins [52–54], protozoan parasites [55], viruses [56], or bacteria [57]. Among these, aptamer-based LIG biosensors are one of the most promising devices, and have been developed for thrombin [58], truncated (recombinant) spike protein [53], and whole virus particles [59], for example.

In this manuscript, we report the development of a biosensor for detection of *L. monocytogenes* using DNA aptamers tethered to platinum-modified LIG electrodes. This is the first reported use of LIG as a low-cost sensor platform for *Listeria* biosensing. First, a literature review was performed to determine available aptamers targeting *L. monocytogenes* from the published literature, and two relevant candidates were selected for testing. Various mixtures of aptamer were tethered to Pt-coated LIG electrodes, and biosensors were tested for *L. monocytogenes* detection under controlled laboratory conditions. The best performing aptasensor arrangement/mixture was then challenged in hydroponic water in a model lettuce system.

## 2 Methods

Two DNA aptamers were selected from the literature for this study. Each aptamer was identified using the whole bacteria SELEX (systematic evolution of ligands by exponential enrichment) after indicating binding with *L. monocytogenes*. Both DNA aptamers target cell-surface proteins likely from the LPxTG protein family. Aptamer A8 has been shown to bind with the invasion LPxTG protein internalin A (InlA) [60] and the aptamer was selected using SELEX. The specific cell-surface target of aptamer LMCA2 is not specifically known [61], as this aptamer was developed using whole-cell SELEX.

### 2.1 Materials and reagents

Thiolated DNA aptamers were purchased from GeneLink, Inc (Westchester, NY). Recombinant InlA from *L. monocytogenes* serotype 4b was obtained from Ray Biotech (Peachtree Corners, GA). Gold sensor chips for surface plasmon resonance were purchased as a kit from Nicoya Life Sciences (Ontario, Canada). Polyimide sheets (2-inch, 0.0025-inch thick, acrylic adhesive) were obtained from McMaster-Carr (Elmhurst, IL). Epson ultra-premium glossy photo paper and nitrocellulose lacquer were purchased from a local store. A mini desktop laser engraver (1000 mW, 1 mm beam with a mean wavelength of $402 \pm 11$ nm) was purchased from HTPOW (London, UK). Nickel-copper alloy tape (100-mm width, 0.13-mm thick, acrylic adhesive) was purchased from Gennel Co. (Beijing, China). Platinum wire (99.95% Pt, 0.5 mm diameter) was obtained from Alfa Aesar (Ward Hill, MA, USA). *L. monocytogenes* real-time PCR assay kits (BAX) were purchased from Hygiena (Camarillo, CA). Actero *Listeria* Enrichment Media was purchased from FoodChex (Alberta, Canada). Sodium hydrogen ferric diethylene-triamine pentaacetate was purchased as Sprint 330 from BASF (Raleigh, NC).

HEPES buffer, Ag/AgCl paint, potassium ferricyanide, potassium ferrocyanide, potassium chloride, calcium chloride, calcium nitrate, ammonium nitrate, potassium nitrate, sodium nitrate, sodium chloride, sodium phosphate (dibasic), magnesium sulfate, sodium molybdate, manganese sulfate, zinc sulfate, copper sulfate, boric acid, potassium phosphate monobasic, potassium phosphate dibasic, magnesium sulfate, chloroplatinic acid, lead acetate, sodium dodecyl sulfate (SDS), EDTA-trypsin, and LB broth were acquired from Sigma-Aldrich (St. Louis, MO, USA). *L. mono* differential agar (77408) was purchased from Merck (Darmstadt, Germany).

### 2.2 *Bacteria* culture

Culture techniques were based on Burrs et al. [62], and are summarized here. *Listeria monocytogenes* (ATCC 19115, serotype 4b) and *Escherichia coli* (ATCC 8739, Crooks) were purchased as food safety test kits (containing pellets, hydrating

fluid and phosphate buffered saline, PBS) from Microbiologics Inc. (St. Cloud, MN). For preliminary affinity testing with surface plasmon resonance, we also tested *E. coli* K12 (ATCC 10798) and *E. coli* O157:H7 (ATCC 43895) according to our previous work [63–66]. Lyophilized pellets of were removed from storage and allowed to equilibrate at room temperature for 30 min. A 2 mL aliquot of hydrating fluid and a 1 L beaker of phosphate-buffered saline (1X PBS, pH 7.4) were pre-warmed in an incubator (37 °C) for 30 min. A pellet of lyophilized bacteria was transferred to 2 mL hydrating fluid. The solution was incubated for 30 min to ensure complete cell hydration. Solution was then transferred to a Pyrex glass culture bottle (in triplicate) containing selective growth media (*L. mono* agar for *L. monocytogenes*; LB broth for *E. coli*). Culture bottles were incubated at 37 °C for 48 h under aerobic conditions.

After incubation, serial dilution series were performed to obtain concentration of $1 \times 10^3$ to $1 \times 10^5$ CFU/mL by dilution with pre-warmed buffer to the desired concentration. Cell solutions were vortex-mixed and concentration was determined by optical density at 600 nm ($OD_{600}$) and confirmed by total aerobic plate counting according to our previous work [40, 41, 67]. Plates were incubated at 37 °C for 48 h and results were recorded as CFU/mL. Biosafety level 2 standards set by the National Institute of Health were used for all experiments.

### 2.3 Localized surface plasmon resonance

Localized surface plasmon resonance (LSPR) was conducted to screen aptamer affinity for recombinant *L. monocytogenes* protein (InlA) and dilute whole bacteria suspensions. An open SPR system from Nicoya Life Sciences (Ontario, Canada) with automatic sensor docking and semi-autonomous injection was used throughout. Two-channel mode was used for all experiments following the protocol provided with the gold sensor chip by Nicoya Life Sciences. In summary, a running buffer was prepared with 50% Tris–HCl, 50% hydroponic solution (pH 7.4) and various amounts of excess $CaCl_2$, as noted. Aptamer disulfide reduction (i.e., decapping) followed the protocol by GeneLink [68], utilizing TCEP (Tris 2-carboxyethyl phosphine hydrochloride) as a reducing agent. In brief, 3% TCEP was mixed with thiolated (capped) aptamer in sterile RNase-free water. The solution was vortex-mixed, and then stored at room temperature for 1 h. The solution was mixed with 3 M sodium acetate until a pH 5.2 was measured, and then 1 mL of absolute ethanol was immediately added, followed by vortex mixing and then storage at −20 °C for 20 min. After this reduction was complete, the solution was centrifuged at 12000 rpm for 10 min, followed by decant in ethanol and air drying of the obtained pellet. The resulting aptamer pellet was used within one hour by dissolving in sterile RNase free water and binding buffer.

Gold LSPR biosensor chips were rinsed three times with Tris–HCl, and then thiolated (decapped) aptamers were covalently attached to gold sensor chips by drop casting a 5 µL aliquot of aptamer solution onto the gold electrode surface and stored in a covered Petri dish at room temperature. The Petri dish was placed on a shaker Table (10 rpm) and allowed to react for 20 min. The biosensor chips were then rinsed three times with Tris–HCl prior to analysis. Running buffer was flushed through the system until a smooth testing baseline was obtained (less than 3% baseline drift). InlA protein serial dilutions were injected into the system from low to high concentration, as noted. For each cycle, a 250 µL sample was flushed through the chip for 5 min at a constant flow rate of 20 µL/min per manufacturer recommendations. Samples (InlA) were injected at least three successive times during testing. To initiate the disassociation step, 0.25% SDS was injected, and signal was monitored for at least 10 min. After the protein disassociation step, fluidic tubing was cleaned with regeneration buffer (HCl pH 2) according to manufacturer recommendations.

For screening aptamers against bacteria targets, fresh microfluidic tubing was used in each experiment, and the system was sanitized prior to analysis with 3% hydrogen peroxide, followed by a rinse in deionized (DI) water. For the association step, a 250 µL aliquot of 100 CFU/mL *Listeria* sample diluted in buffer was injected for the association step, followed by injection of 0.25% EDTA-trypsin supplemented with 0.25% SDS to initiate the disassociation step. LSPR analysis at bacteria concentrations greater than 100 CFU/mL was not possible due to persistent clogging of microfluidic tubing. After analysis of bacteria association, microfluidic tubing was replaced, and the system was flushed for one hour with regeneration buffer. Kinetic parameters were calculated using Trace Drawer software (Nicoya Life Sciences) and verified with manual calculation in Excel.

### 2.4 Nanoplatinum-coated LIG electrode fabrication

Step-by-step details for fabrication of LIG electrodes are provided in our published protocol [69]. Briefly, Kapton tape was adhered to Epson ultra-premium glossy photo paper, which was used as a backing material for LIG electrodes. The polyimide film was carbonized with a 1000 mW Mini Laser Engraver (405-nm wavelength LED), as described in our previous

work [51, 70]. The physical area of the LIG working electrodes was 5 mm. Electrode stems were passivated with lacquer and then metal tape was fixed to the bonding pads.

Pulsed sonoelectrodeposition (pulSED) of platinum (nPt) was used to metallize the working electrode based on Taguchi et al. [71]. A plating solution of 0.72% (v/v) chloroplatinic acid and 0.001% (w/v) lead acetate was prepared, and electrodes were immersed for room temperature deposition. A preliminary study was conducted to determine an appropriate sonication time (0.1 s), plating time (1.0 s), and number of pulSED cycles (30) based on visual inspection and determination of electroactive surface area. The total plating time was 30 s.

### 2.5 Biofunctionalization of electrodes with aptamer

Aptamers were stored in a −10 °C freezer when not in use. After thawing at room temperature for 30 min, aptamers were reconstituted in 100 µM TE buffer (10 mM Tris, 1 mM EDTA; pH 7.5) and decapped following manufacturer protocol [68]. Each aptamer was diluted to a working concentration of 1.0 µM in reconstitution buffer. For biofunctionalization, platinized LIG (nPt-LIG) were rinsed with DI water three times, air dried at room temperature for 30 min, and then 5 µL of thiolated aptamer solution was drop cast onto the working electrode. Electrodes were stored for 2 h at room temperature in a covered Petri dish to allow DNA adsorption. Functionalized electrodes were rinsed three times with buffer, and then stored in a Petri dish at 4 °C until used (within 48 h).

A single factor design with multiple levels was used to test the effect of the aptamer solution composition (3 levels: 1 µg A8/ml, 1 µg LMCA2/ml, and [0.5 µg A8 + 0.5 µg LMCA2]/ml) on the electrochemical detection performance of the biofunctionalized electrodes. The response variables were impedance and capacitance obtained from electrochemical impedance spectroscopy analysis. All biofunctionalization experiments were performed in triplicate.

### 2.6 Electrochemical analysis

Cyclic voltammetry (CV) and electrochemical impedance spectroscopy (EIS) were used as described in our previous work [41, 72–74], and detailed in our published protocol [75]. Individual voltammograms were analyzed by fitting a polygon (absolute area) representative of the area between the anodic and cathodic sweeps (ABC). The calculated value of ABC for each curve is given in the supplemental.

Applying the calculated values of ABC for each CV curve, specific capacitance ($C_p$) and charge (Q) were calculated based on Li et al. [76] (Eqs. 1, 2, 3), where m = mass of LIG (approximately 0.1 g), v = scan rate, and dE = change in potential.

$$\int_{E_1}^{E_2} I(v)dv = \int_{E_1}^{E_2} \left(C_p * m * v\right)dE \tag{1}$$

The area between the anodic and cathodic time series curves (ABC) was used to calculate the value of $C_p$, which represents the net sum of the charging and discharging portions of the CV sweeps. In other words, ABC is the difference between the charging current and discharging current is $C_p$, where DE = the potential window of the CV scan.

$$C_p = \frac{ABC}{2m * v(\Delta E)} \tag{2}$$

$$Q \propto \frac{ABC}{\Delta E} \tag{3}$$

Log–log transforms (Eq. 4) were used to assess whether the electrode behavior was under capacitive or diffusion control as shown by Li et al. [76]. In summary, if peak anodic or cathodic current ($i_p$) is proportional to the scan rate ($v$) for a completely reversible diffusion-limited process, the parameter (b) in Eq. 4 is equal to 1.0. If, on the other hand, the response of the electrochemical cell is controlled by capacitive processes under the conditions tested, the value of the coefficient b will be between 0.5 and 1.0.

$$log\left(i_p\right) = log(a) + blog(v) \tag{4}$$

Electroactive surface area (ESA) was calculated using Cottrell plots based on the Randles–Sevcik theorem (Eq. 5), where $i_p$ is peak current, D is the diffusion coefficient, C is the concentration of redox probe(s), and v is the scan rate.

$$i_p = 2.69X10^5 * n^{1.5} * D^{0.5} * C * ESA * v^{0.5} \quad (5)$$

Heterogenous electron transfer (HET) coefficient was calculated using the Nichols transform as described in our previous work [51] using Eqs. 6 and 7, where y is the dimensionless charge transfer coefficient, g is the dimensionless quantity $D_0/D_R$, a is the transfer coefficient, $k_s$ is the HET constant, F is the Faraday constant, R is the universal gas constant, and T is the temperature.

$$\psi = \frac{\gamma^a * k_s}{(\pi * a * D_0)^{0.5}} \quad (6)$$

$$a = \frac{n * F * v}{RT} \quad (7)$$

All EIS measurements were conducted in a solution of 2.5 mM potassium ferricyanide (III), 2.5 mM potassium ferrocyanide trihydrate, and 100 mM potassium chloride. Analysis was conducted using a three-electrode setup in an EA163 potentiostat and an ERZ100 Electrochemical Impedance Analyzer from eDAQ Inc. (Colorado Springs, CO). The scanned frequency ranged from 0.1 Hz to 100 kHz with an applied DC potential of 250 mV and an AC amplitude of 10 mV. Where noted equivalent circuit modeling was conducted with ZMAN 2.2 (WonATech) software.

### 2.7 Analytical performance characterization

Electrochemical detection performance of the aptasensors was determined via EIS. A 400 µL aliquot of PBS containing bacteria was drop cast onto the aptasensor. A 5 min equilibration time was used, followed by rinsing with DI water three times. After acquisition of EIS data, cutoff frequency analysis was performed using impedance and capacitance data. Calibration curves were prepared by analyzing response between 1 CFU/mL and $10^5$ CFU/mL. Analytical sensitivity was defined as the slope of the linear portion of the calibration curve of aptasensor output vs. bacteria concentration. For selectivity testing, the change of output signal from the aptasensor exposed to *L. monocytogenes* (positive control) was contrasted against the change of output signal from the aptasensor exposed to *E. coli* (Crooks, K12, O157:H7) at several concentration levels.

Testing procedures were based on our previous work for other bacteria biosensors used in hydroponic systems [43, 57, 63]. In summary, a portable potentiostat [77] was used to conduct EIS in lettuce trial water quality analysis. Data acquisition and control used a Samsung tablet connected to the potentiostat via Bluetooth (ABE STAT app available from Google Play). Commercial Ag/AgCl reference electrodes and platinum wire counter electrodes were used. At each calibration point tested (baseline 0, 1, 10, 100, and 500 CFU/ml), three EIS measurements were taken for each biosensor to account for any drift due to dielectric charge/discharge or Ohmic drop. The biosensor testing output was the mean of these triplicate measures. For calibration curves, analytical sensitivity was calculated as the linear slope using various response variables, as noted. LOD was calculated using the three-sigma method (99% confidence) [78].

### 2.8 Aptasensor validation

To demonstrate the usability of the develop aptasensor as a diagnostic tool for agricultural applications, a hydroponic lettuce system was contaminated with bacteria based on Sidhu et al. [40] and Giacobassi et al. [63]. Briefly, a 65 L aeroponic system was used to grow lettuce from plugs obtained from a greenhouse in Gainesville, FL. Foam plugs of one week old hydroponic lettuce (*Lactuca saliva*) were transferred to CocoTek-lined mesh plastic seed cups and then filled with expanded clay pellets (Mr. Stacky Hydroponic Center, Lake City, FL, USA). Full spectrum light-emitting diode (LED) grow lights (75 W equivalent) were positioned 2 m above the system and a timer was set for photoperiod of 8 h. Sterilized nutrient solution (see supplemental section) was replaced every 7 days. Five days prior to testing, the hydroponic system was inoculated with a 1 mL aliquot of $10^8$ cells/mL and re-inoculated every day with fresh inoculum for three consecutive days (4 days total). On the day of testing (i.e., 5th day), the water was analyzed (total of 24 h between the last inoculation and the testing).

All samples from hydroponic system were tested for presence of *L. monocytogenes* using both the developed aptasensor and also AOAC-approved real time PCR kits. For aptasensor testing, a 10 mL sample was taken from the hydroponic system, and tested with no enrichment. PCR was used as the gold standard technique for cross-validation of aptasensor

test results. In brief, *Listeria* enrichment media was used to prepare bacteria inoculums by incubation at 35 °C for 20–24 h. To conduct the PCR test, 150 µL protease was mixed with 12 mL lysis buffer, and then 200 µL lysing agent was added. This mixture was added to reagent tubes and then 5 µL of sample was added. A PCR block was pre-heated to 55 °C and cooling blocks were stored at 4 °C. The sample/reagent was held at 55 °C for 30 min, and then ramped to 95 °C for 10 min. Reaction vials were immediately transferred to cooling blocks and stored for 5 min. The samples were added to the rack according to the rack file provided by the software, and auto-program for *L. monocytogenes* was selected. PCR cluster tubes and samples were arranged in the cooling block and tablets were hydrated with 30 µL lysate buffer, then allowed to hydrate for 10 min. The Q7 cycler was initialized, and the software returned qualitative positive/negative values for each of the 96 wells (as well as Ct curves). No signal errors occurred for qualitative analysis of these samples.

### 2.9 Diagnostic index

Youden index (J) was used to estimate the potential effectiveness of the developed aptasensor as a dichotomous diagnostic tool for *in-situ* detection of *L. monocytogenes* in hydroponic operations. The diagnostics performance and Youden index were calculated using true positive (TP), true negative (TN), false positive (FP), and false negative results obtained from comparing the diagnostic test outcome (2×2 contingency table) to PCR results as shown in Eqs. 8, 9, 10, 11 [79–81].

$$Accuracy(\%) = \frac{TP + TN}{total} * 100 \tag{8}$$

$$Sensitivity(\%) = \frac{TP}{TP + FP} * 100 \tag{9}$$

$$Specificity(\%) = \frac{TN}{TN + FN} * 100 \tag{10}$$

$$Youden\ index = Sensitivity + Specificity \tag{11}$$

### 2.10 Statistical analysis

All experiments were performed in triplicate. Where relevant, average results are shown as mean, where error bars represent the standard deviation. All statistical analysis was conducted in R Studio (Boston, MA). Analysis of variance (ANOVA; $p < 0.05$) was conducted to determine statistical significance of noted differences; independence, and normality. Variance homogeneity was analyzed using residual plots. Where necessary, data was LOG (natural or log-10) transformed and re-analyzed using ANOVA and Tukey tests. For initial screening analysis, ANOVA without replication was performed using DataTab, analyzed using both paired and unpaired assumption.

Details of hydroponic solution, material imaging analysis, electrochemical characterization of materials, equivalent circuit modeling results, and diagnostic testing in hydroponic water are provided in the supplemental section. Where relevant, reference is provided to relevant detailed (step-by-step) protocols published by our team [70, 75].

## 3 Results and discussion

SEM images indicated a macroscopic stitched pattern with nano/microscale coral features that have been reported by others in recent material studies of LIG [52, 73, 82, 83] (see supplemental section). Raman spectra and FTIR (with and without metallization) have been shown in our previous work [51].

### 3.1 Affinity screening

Target (InlA) binding was screened for select aptamers using a truncated (recombinant) target protein based on an approach similar to Ullah et al. [84]. Figure 1 shows results of affinity screening using localized surface plasmon resonance (LSPR) in a flow through system from Open SPR. When supplemented with calcium, aptamer A8 had a high affinity

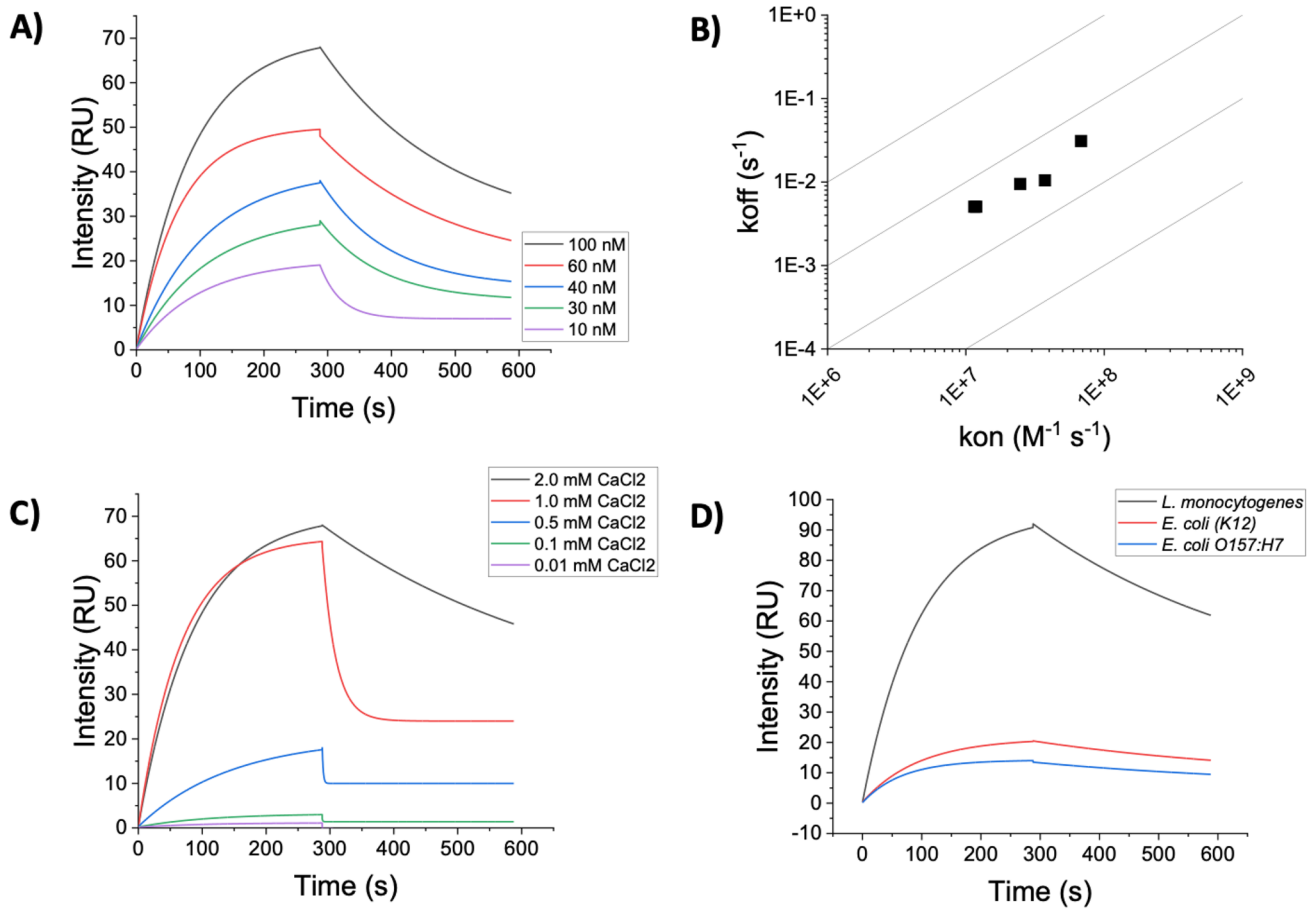


**Fig. 1** Preliminary screening of aptamer A8 toward InlA and intact bacteria **A)** Interaction sensogram for aptamer A8 and InlA in 1 mM $CaCl_2$, 50% Tris–HCl, and 50% hydroponic solution at room temperature. Concentrations of InlA noted in legend. **B** On–off binding map for aptamer A8 versus InlA based on data in panel A. **C** Effect of calcium chloride concentration on InlA binding by aptamer A8. **D** Whole cell testing of aptamer A8 versus *L. monocytogenes* and two strains of *E. coli*. at a cell concentration of 100 CFU/mL

toward recombinant InlA and also intact *L. monocytogenes* (relative to *E. coli*). Figure 1A shows a representative plot for aptamer A8 interacting with InlA in 1 mM $CaCl_2$, 50% Tris–HCl, and 50% hydroponic solution at room temperature. A well-defined association phase was recorded for InlA concentrations from 10 to 100 nM (20 µL/min flow of binding buffer). After injection of the disassociation buffer (0.25% SDS), InlA was displaced at all concentrations tested. The association and disassociation plots were auto-adjusted for peak shifts using the instrument software. On–off binding maps for aptamer A8 indicate an affinity constant ($K_D$) for InlA in the range of 10–20 nM (Fig. 1B). The experiment was repeated for aptamer LMCA2. However, no binding was observed for recombinant InlA protein (data not shown). Aptamer A8 binding with InlA was challenged using different supplementations of the calcium chloride concentration in the binding buffer (Fig. 1C). For $CaCl_2$ concentrations between 0.1 and 1 mM, the peak association was linear ($R^2 > 0.95$), with a saturation affect outside of this range. Aptamer A8 was challenged against intact bacteria (Fig. 1D), including *L. monocytogenes* and two strains of *E. coli* (250 µL aliquots at a concentration of 100 CFU/mL). The association with *L. monocytogenes* was at least five times higher than *E. coli* (K12 and O157:H7), and the disassociation was 7 times slower, indicating selective binding between aptamer A8 and InlA on *L. monocytogenes*. Whole cell analysis for LMCA2 was similar, with higher intensity and association ($k_{on}$).

Aptamers were further screened for detection of *L. monocytogenes* using EIS. Qureshi et al. [85] showed electrochemical affinity screening with EIS is comparable to classic competition assays. Figure 2. shows representative plots of EIS data for each of the three aptamer coatings in the presence of $10^3$ CFU/mL *L. monocytogenes* in hydroponic water. Phase diagrams (Fig. 2A) indicate a pseudo-capacitive behavior for all three aptamer coatings. The maximum negative phase was between 0.1 Hz and 0.5 Hz for all coatings, and highest for the 50/50 mixture of aptamers. The phase plots show a stable pseudocapacitive behavior at low frequency (between 0.1 to 1 Hz). Distinct low frequency behavior for each aptamer

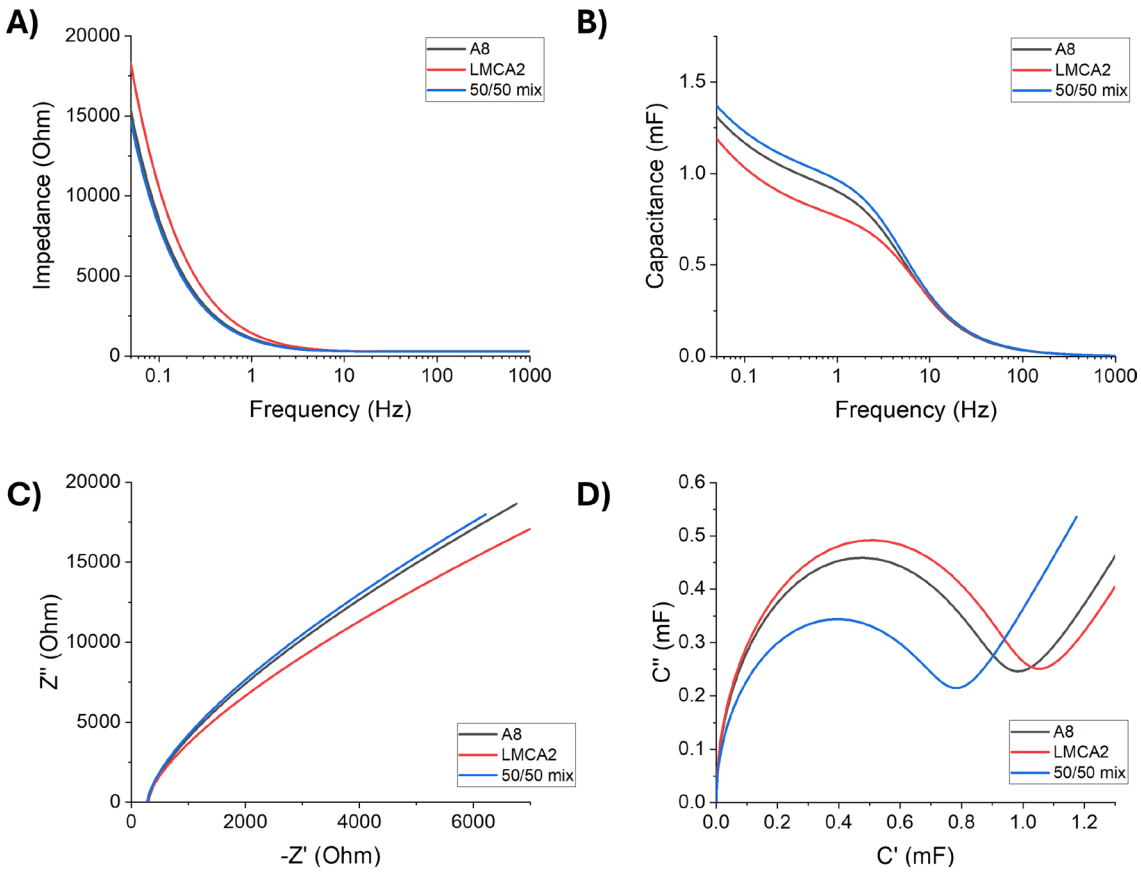


**Fig. 2** Electrochemical screening of aptamers for targeting *L. monocytogenes* ($10.^3$ CFU/mL) using EIS. Representative plots for: **A** Bode impedance, **B** Bode capacitance, **C** Nyquist impedance, and **D** Nyquist capacitance. All experiments used 50% lettuce hydroponic water supplemented with buffer (0.5 mM total divalent cation concentration)

toward *L. monocytogenes* is shown in Fig. 2B. The magnitude of the capacitive signal is highest below a frequency of 1 Hz. This observation aligns with conventional theory which predicts that capacitance should dominates the EIS signal at low frequency (conversely resistance terms dominate the signal at high frequency) [86]. Results from equivalent circuit modeling (diffusion-limited RC circuit) are shown in the supplemental section for comparison. Nyquist plots (Fig. 2C-D) indicate diffusion-limited behavior with negligible relative change in solution resistance (see supplemental section for $R_s$, $R_w$, $R_{ct}$, and $C_{dl}$ analysis using Randles-Ershler model). These plots indicate a difference in each aptamer coating, particularly for the measured capacitance (Fig. 2B and D). Previous whole cell biosensors on LIG-metal electrodes also indicated capacitive behavior [52, 59].

Impedimetric or capacitive response at in the low frequency (AC) range (0.01 to 10 Hz) were analyzed to compare the percent change in signal at baseline and in the presence of target cells. In this low frequency region, the 50/50 aptamer mixture and LMCA2 aptamer showed the highest analytical sensitivity toward intact cells (Fig. 3A-B), although ANOVA indicated no statistical difference between the analytical sensitivity for the LMCA2 and the 50/50 mixture for this screening test using $10^3$ CFU/mL as a test concentration. Use of 0.5 Hz as a cutoff frequency resulted in the highest SNR for acquisition of capacitance; impedimetric response was optimum at 0.1 Hz. Both signal change and SNR were significantly higher for impedimetric response. There was no statistical difference in the SNR for impedance or capacitance as the response variable for the LMCA2 aptamer or the 50/50 aptamer mixture. Results of equivalent circuit modeling (charge transfer resistance and double layer capacitance) further support these data (*see supplemental* Sect. 4).

To further explore the EIS screening at a cell concentration of $10^3$ CFU/mL, calibration curves were prepared in the range of 1 to $10^5$ CFU/10 mL. Bode impedance and capacitance plots show detection of *L. monocytogenes* at low AC frequency (0.1 or 0.5 Hz Hz), but poor response at 1.0 Hz (Fig. 4A-B). The optimum cutoff frequency varied, depending on which response variable was used. For impedimetric sensing, the sensitivity was highest at a frequency of 0.1 Hz (Fig. 4A), while for capacitive sensing, the highest sensitivity was at 0.5 Hz (Fig. 4B). For these optimum cutoff

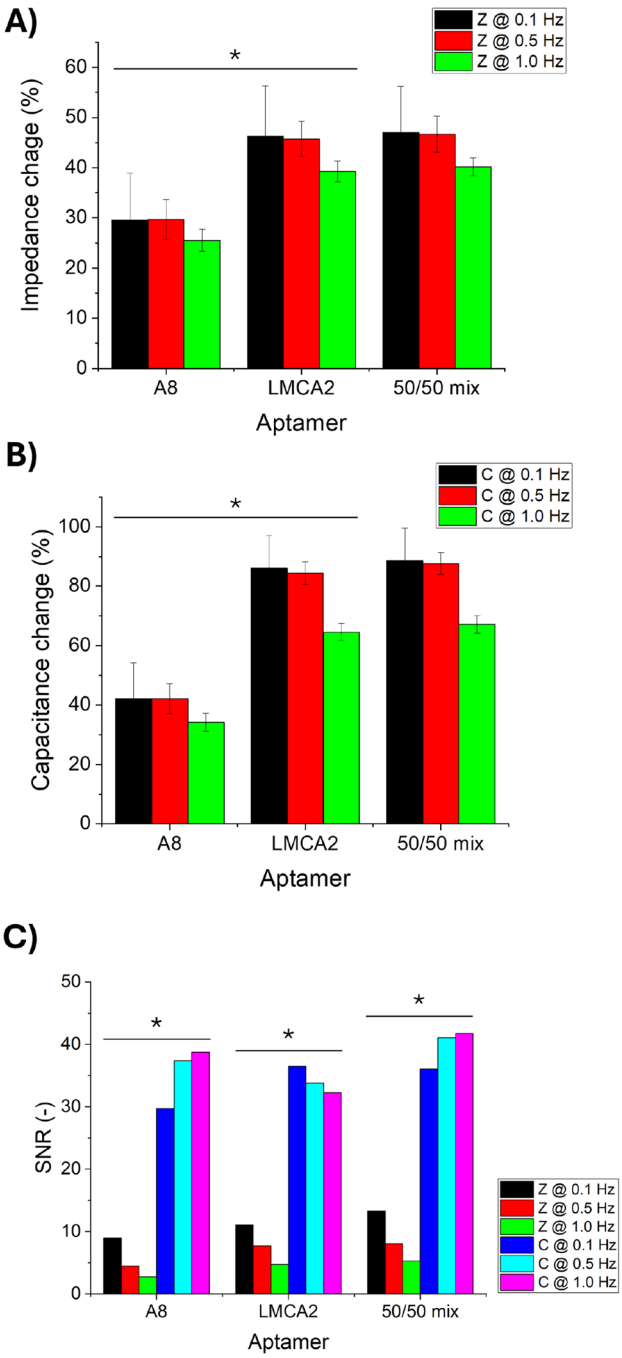


**Fig. 3** Cutoff frequency analysis of impedance spectra in hydroponic water supplemented with buffer (0.5 mM total divalent cation concentration). Spectra were analyzed at baseline and in the presence of *L. monocytogenes* ($10.^3$ CFU/mL). Average plots for: **A** Change in impedance, **B** Change in capacitance, and **C** Signal to noise ratio (SNR). All experiments were repeated in triplicate; error bars represent standard deviation of the mean. Horizontal lines with asterisk indicate groups which were statistically different (a = 0.05)

frequencies, the sensitivity toward *L. monocytogenes* was highest for the 50/50 aptamer mixture, followed by aptamer LMCA2 (Fig. 4C-D). The highest concentration tested was $10^5$ CFU/10 mL. The maximum $R^2$ value was for impedimetric sensing at 0.1 Hz ($R^2 = 0.86$; see supplemental Table S4 for all experiments).

The LOD was lowest when using the 50/50 aptamer mixture, resulting in a LOD of 16 CFU/10 mL for impedance at 0.1 Hz and 11 CFU/10 mL for capacitance at 0.5 Hz (Fig. 4E). The SNR was highest for the 50/50 aptamer mixture with capacitance at 0.5 Hz (Fig. 4F). The biosensor was linear up to a concentration of $10^5$ CFU/mL, regardless of the response variable or cutoff frequency (see supplemental Table S4 for details).

Equivalent circuit modeling was conducted to analyze the Randles-Ershler circuit model. The trends were similar to use of impedance or capacitance as response variable (see supplemental Figure S.4.3), although the variability was relatively high when using charge transfer resistance (from equivalent circuit modeling. In addition, the LOD and sensitivity were both relatively poor using equivalent circuit modeling. Taken together, these data indicate that

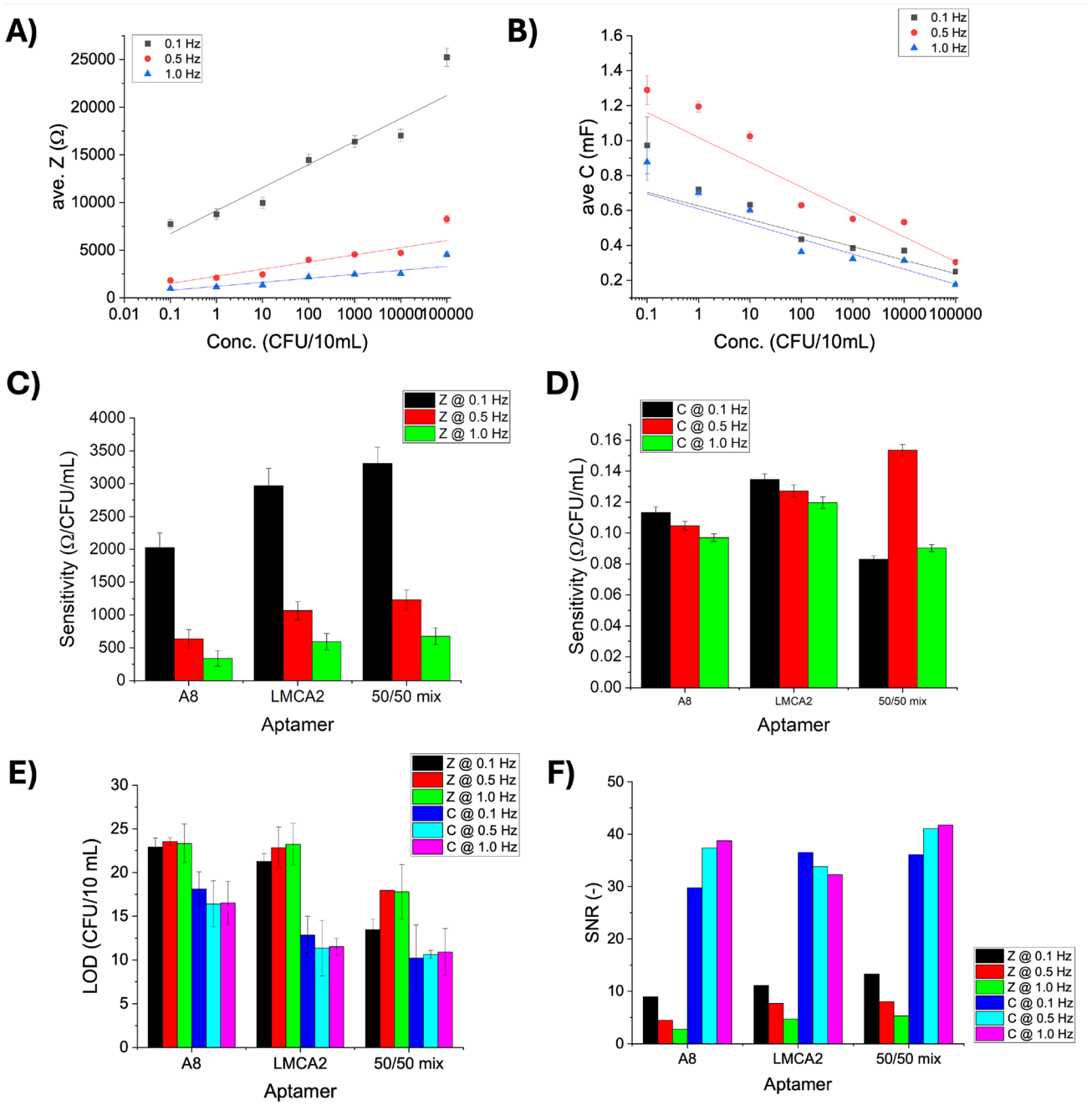


**Fig. 4** Calibration of capacitive aptasensor for *L. monocytogenes* in hydroponic water using 50/50 aptamer coating mixture. Representative plots showing calibration curves at three cutoff frequencies using: **(A)** impedance and **(B)** capacitance. Average analytical sensitivity (Ω/CFU/mL) for replicate electrodes using: **(C)** impedance and **(D)** capacitance as response variable. **(E)** Limit of detection (CFU/ 10 mL calculated for different coating (A8, LMCA2, 50/50 mix) at various cutoff frequencies; **(F)** Signal-to-noise ratio for different coating. All error bars represent standard deviation of the mean (n = 3 replicates)

the aptasensor operates more efficiently as a capacitive biosensor at 0.5 Hz. To challenge this, a selectivity test was carried out.

### 3.2 Selectivity toward *L. monocytogenes*

Figure 5 shows the calibration *toward L. monocytogenes* and selectivity over *E. coli* (Crooks) in hydroponic water (10 mL samples). Full performance characterization is shown in the supplemental section. Figure 5A shows the response using

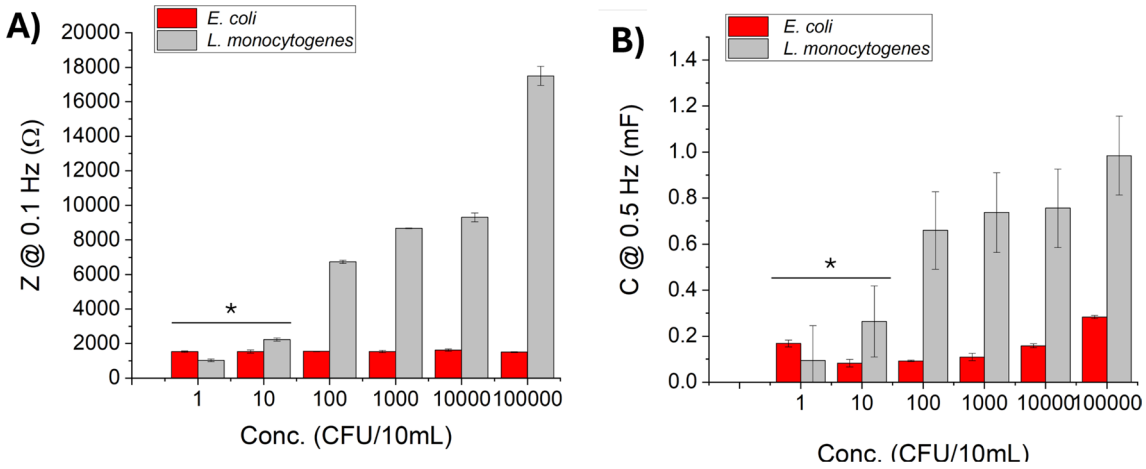


**Fig. 5** Selectivity testing in hydroponic water using different response variables: **A** Impedance at 0.1 Hz and **B** Capacitance at 0.5 Hz. All experiments were repeated in triplicate; error bars represent standard deviation of the mean. Horizonal lines with asterisk indicates groups that were not statistically different (a = 0.05)

impedance at 0.1 Hz; Fig. 5B shows the data for capacitance at 0.5 Hz. The ratio of mean signal to standard deviation is lower for capacitive response (relative to impedance at 0.1 Hz), indicating capacitance is not the optimal response variable. The ratio of mean response toward *L. monocytogenes* compared to *E. coli* using impedance at 0.1 Hz (ratio = 6.5) was higher than the response for capacitance at 0.5 Hz (ratio = 1.3).

For all samples with a concentration of 10 CFU/10 mL or higher, the capacitance was two to three times higher than the response for *E. coli (Crooks)*, but the SNR was relatively low (indicated by the high standard deviation).Near the LOD (10 CFU/10 mL), the capacitance was three times higher for *L. monocytogenes* than *E. coli*, but the standard deviation for capacitive response was considerable higher than impedimetric response (i.e., lower SNR). There was no significant difference between background and 1 CFU/10 mL for any test. In part, this lack of selectivity at low concentration may have been due to the serial dilution methods used, and the sample analysis method.

At concentrations greater than 100 CFU/mL, the impedance signal was at least 4 times higher for *L. monocytogenes* compared to *E. coli*. However, near the LOD the impedance reading was not significantly different for the two species, indicating no specificity. This important detail is not commonly discussed in the literature and is an important aspect when reporting LOD values. In a mixture potentially containing more than one species of bacteria, these data suggest that a more appropriate LOD is 100 CFU/10 mL (although the classic calculation in a single bacteria calibration suggests the LOD is ten times lower).

### 3.3 Challenge study in hydroponic system during lettuce cultivation

The hydroponic system was inoculated with *L. monocytogenes* and operated continuously for 48 h according to Sidhu et al. [40]. Water samples were collected from the system and analyzed using both PCR and aptasensors. Use of multi-aptamer (50/50 mixture) targeting *L. monocytogenes* significantly improves detection accuracy. Table 1 shows the

**Table 1** Key performance indicators for *L. monocytogenes* detection in lettuce hydroponic water using EIS (n = 3 replicate tests; errors represent standard deviation of the mean)

| Aptamer coating | Youden index (J) (accuracy) | Analytical sensitivity | | LOD [CFU 10 $mL^{-1}$] | |
|---|---|---|---|---|---|
| | | Z @ 0.1 Hz [W-log $CFU^{-1}$-µL] | C @ 0.5 Hz [mF-log-$CFU^{-1}$-mL] | Z @ 0.1 Hz | C @ 0.5 Hz |
| A8 | J = 0.20 (43%) | 2024 ± 226 | 105 ± 13 | 22 | 16 |
| LMCA2 | J = 0.73 (81%) | 2968 ± 368 | 127 ± 4 | 21 | 11 |
| A8/LMCA2 | J = 0.77 (86%) | 3309 ± 329 | 154 ± 7 | 16 | 10 |

All tests were performed in 50% lettuce hydroponic water

diagnostic performance of the aptasensor toward *L. monocytogenes* in hydroponic water. Details for truth tables are shown in Table S4.3 to S4.7.

Figure 6 shows contingency diagrams (visualization of 2 × 2 truth tables) for the diagnostic analysis versus PCR (using methods based on Moreira et al. [56]). The analysis is shown for capacitance at 0.5 Hz as the response variable, based on the analysis shown in Fig. 3, 4, 5. For all diagrams, the blue regions in the contingency plots indicate prevalence of false negatives, while red indicate false positives. Aptamer A8 and LMCA2 (Fig. 6A, B) plots show relatively high false negatives (which is the worst-case test result for a pathogen biosensor). The mixture of aptamer A8 and LMCA2 had the highest accuracy (85.7%) and Youden J (0.77) than either aptamer separately, but Fig. 6C shows that this improvement was also associated with additional false positive results. For pathogen sensing, this is not as consequential as a false negative, which is why the Youden J and accuracy are both higher. Figure 6D shows the results of the PCR test, which also indicate a false positive in one of the samples. During initial screening, scrambled aptamers showed poor diagnostic performance and calculation of accuracy was not possible. Detailed information is included in the appendix (supplemental Sect. 4), including Wilson confidence intervals (95% confidence). Additional studies are required to analyze the sensor response when testing mixtures of various bacteria, including other strains/species not tested here (e.g., *L. ivanovii, L. innocua).*

Numerous cell-surface proteins on *L. monocytogenes* are potential targets for aptamers [87, 88] (see schematic in supplemental Sect. 5). One of the DNA aptamers in this study (A8) is known to bind the invasion protein InlA, which

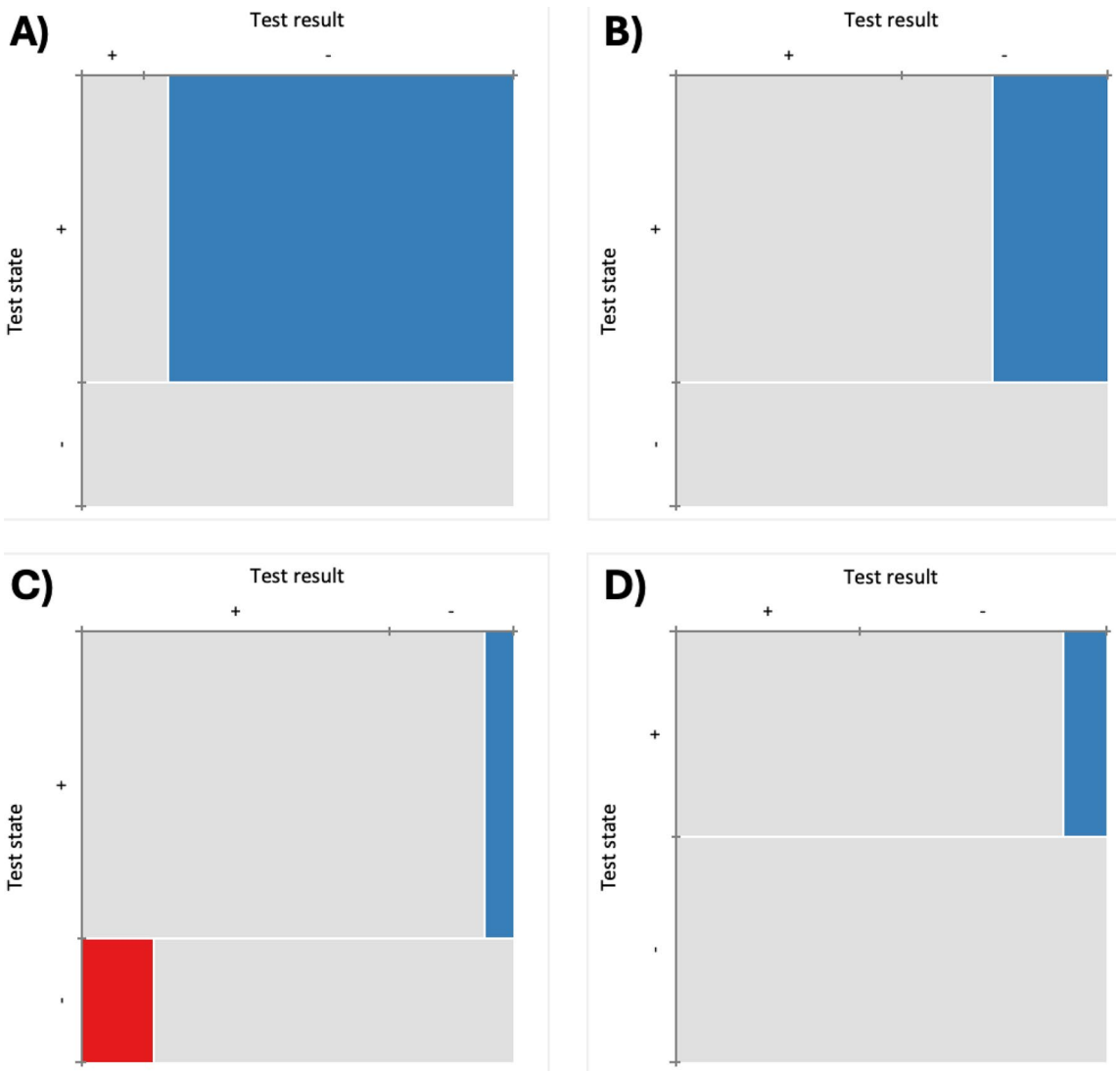


**Fig. 6** Platinum-coated LIG aptasensors compared to PCR as gold standard. **A** Aptamer A8, accuracy = 42.9%, Youden J = 0.20; **B** Aptamer LMCA2, accuracy = 81.0%, Youden J = 0.73; **C** Aptamer A8/LMCA2 mix, accuracy = 85.7%, Youden J = 0.77; and **D** PCR test, accuracy = 96%, Youden J = 0.94. Blue regions indicate prevalence of false negatives, and red indicate false positive

was confirmed in this work (see Fig. 1). The aptamer was developed using traditional SELEX processes and has been validated in optical and electrochemical device testing. InlA is also present in other *Listeria* species such as *L. ivanovii*, which highlights the importance of more selectivity studies required for these types of biosensors. The second aptamer in this study (LMCA2) did not bind recombinant InlA in this study (LSPR data) but was highly selective for *L. monocytogenes* over *E. coli* in the electrochemical LIG sensor (see supplemental Sect. 4 for details). Identification of the specific target for aptamer LMCA2 requires additional research, but our results confirm the results by Lee et al. [61] showing affinity for *L. monocytogenes* (the aptamer was developed using whole-cell SELEX, which is a relatively new approach). Interestingly, the combination of these two aptamers resulted in the highest accuracy in hydroponic media (86%), demonstrating the applicability of this concept in whole cell detection.

Mixed aptamer systems have been used in other research for targeting small molecules. Liu et al. [89] utilized colorimetric displacement assays to study multi-aptamer targeting of small molecules (cathinones). To our knowledge, multi-aptamer targeting of intact bacteria has not been explored. This work demonstrated that multi-aptamer systems have lower cross reactivity when compared to single aptamer systems. Other sensor performance indicators may also be improved. Drabovich et al. [90] utilized a tri-aptamer system to extend the working range of a fluorescent protein detection system. Improving dynamic range may be the most common goal of multi-aptamer sensor systems. Pan et al. [91] reviewed the use of multi-aptamer systems for improving the dynamic sensor range based on redox-labeled bioprobes with electrochemical transduction for signal acquisition. The range of targets which have been explored using this approach include small molecules, peptides, and phospholipids (vesicles).

Given the large surface area of living cells, together with the diversity of extracellular targets amenable to aptamer interaction, mixed aptamer systems may be an effective strategy for improving diagnostic performance in complex media. Here, we have demonstrated the feasibility of the multi-aptamer approach for development of label-free aptasensors targeting a Gram-positive bacterial pathogen commonly found in contaminated food.

### 3.4 Comparison of *L. monocytogenes* biosensors

A summary table of impedimetric biosensors in the published literature is shown in Table 2**.** The limit of detection (10 CFU/10 mL) and response time (12 min) of the aptasensor reported here are competitive with other aptasensor and immunosensor devices in the literature. The response time includes sampling and all sensor signal acquisition. Although beyond the scope of this manuscript, Qian et al. [66] recently developed a machine learning model for autonomous analysis of biosensor data for pathogen detection in irrigation water which could be used to include data analysis within this 12 min testing time. For *L. monocytogenes*, most food safety regulations require a solid food sample of 25 g is tested after stomacher bag pretreatment. For irrigation water, the regulations are not as defined, but a zero-tolerance policy for *L. monocytogenes* detection may be appropriate for fresh produce production systems [92]. In this study, we analyzed 10 mL samples, which is a step toward processing relatively large volumes (this sample volume was higher than all published sensors reported in Table 2). Testing water sample volumes greater than 1 mL is of upmost importance for obtaining data which is representative of the hydroponic system. While the 10 mL samples in this study are a step in the right direction, further research is required to extend this to the 1001 mL goal established in other studies [93–95]. Although Radhakrishnan et al. [96] reported a lower LOD (5 CFU $mL^{-1}$) than the work here (sensor was tested in diluted tomato extract), the exposure time and accuracy were not reported. Further, only small volumes of sample were tested. Sidhu et al. [40] developed an interdigitated platinum electrode (Pt-IDE) aptasensor with a LOD of 5.4 CFU $mL^{-1}$ and a sensitivity $0.27 \pm 0.03$ kΩ/log CFU-$mL^{-1}$ in diluted vegetable broth. However, the sensor was only tested toward *L. innocua* and the accuracy was not reported.

Chemburu et al. [97] developed an amperometric test based on carbon dots with an antibody + enzyme cap that was able to detect *L. monocytogenes* as low as 10 CFU-$mL^{-1}$ in PBS buffer. However, the test failed to achieve the same LOD in real food samples and accuracy was not reported. Ding et al. [98] demonstrated a LOD of 10 CFU-$mL^{-1}$ in TBS buffer based on a potentiometric biosensor using aptamer as capture material and protamine as blocking agent. The device showed a response time of 40 min and included a polycation sensitive membrane electrode, although accuracy was not reported.

Aptasensors achieve excellent performance indicators (sensitivity, LOD, response time, accuracy) for *L. monocytogenes* detection in food samples. The most important contribution of this work is direct comparison of the biosensor to gold standard analysis (PCR), facilitating the calculation of diagnostic accuracy (86% in this study). Other manuscripts in the literature shown in Table 2 do not include this validation step, thus direct comparison is not possible.

**Table 2** Performance comparison of impedimetric *Listeria* biosensors for food samples (adapted from Hills et al. [43])

| Biosensor | Samples tested | Analytical Sensitivity | Range [CFU-mL$^{-1}$] | Time [min] | Accuracy [%] | Reference |
|---|---|---|---|---|---|---|
| Nanobrush Aptasensor | Buffer | 3.6 ± 0.2 kΩ/log CFU-mL$^{-1}$ | 3 to $10^7$ | 17 | NR | Hills et al. [43] |
| Nanobrush Immunosensor | Buffer | 3.1 ± 0.3 kΩ/log CFU-mL$^{-1}$ | 3 to $10^7$ | 17 | NR | Hills et al. [43] |
| Nanobrush Aptasensor | Vegetable broth | 3.8 ± 0.2 kΩ/log CFU-mL$^{-1}$ | 9 to $10^2$ | 17 | NR | Hills et al. [43] |
| Nanobrush Immunosensor (mAb) | Vegetable broth | 2.7 ± 0.4 kΩ/log CFU-mL$^{-1}$ | 16 to $10^4$ | 17 | NR | Hills et al. [43] |
| Pt-IDE Aptasensor | Vegetable broth | 0.27 ± 0.03 kΩ/log CFU-mL$^{-1}$ | 5 to $10^6$ | 17 | NR | Sidhu et al. [40] |
| Gold Electrode Immunosensor | Tomato Extract | 1.1 ± NR kΩ/log CFU-mL$^{-1}$ | 5 to NR | * 3 | NR | Radhakrishnan et al. [96] |
| Carbon dots with Ab/enzyme cap | Buffer | 0.0021 μA/CFU-mL$^{-1}$ | 10 to $10^6$ | 30 | NR | Chemburu et al [97] |
| Polycation sensitive membrane electrode with aptamers and protamine (E) | Buffer | 0.19 mV/CFU- mL$^{-1}$ | 10 to $10^5$ | 40 | NR | Ding et al. [98] |
| nAu-pAb Immunosensor | Lettuce (spiked) | NR | 300 to $10^6$ | 120 | NR | Wang et al. [99] |
| IDE nAu-pAb Immunosensor | Lettuce | NR | $10^3$ to $10^7$ | 180 | NR | Kanayeva et al. [100] |
| Impedimetric aptasensor @ 0.5 Hz (multi-receptor) | Hydroponic water (lettuce) | 154 ± 4 mF / log CFU-mL$^{-1}$ | 10 to $10^5$ | 12 | 86% | *This work* |

*Range = Reported LOD and upper limit of calibration*

*Time = response time (including incubation/preconcentration)*

*NR = not reported*

* *Incubation and exposure time not reported*

*nAu = gold nanoparticle*

*pAb = polyclonal antibody*

*mAb = polyclonal antibody*

### 3.5 Biosensors as a decision-making support tool for food safety

In the US, the responsibility of designing and implementing a *L. monocytogenes* monitoring program is the burden of the food producer. At a minimum, monitoring programs must regularly test foods and the processing environment for the presence of *Listeria* spp (e.g., indicator species). Cross-contamination is a leading cause of outbreaks associated with minimally processed foods such as fresh produce [101–103]. Food contact zones and non-food contact surfaces must be monitored at specified time intervals for pathogens and indicator microorganisms [104–106]. The food industry faces a critical balancing act due to the asynchronous nature of environmental monitoring, holding product while waiting for test results, and the risk of disease outbreak if inventory must be transported to prevent loss of revenue due to perishability of fresh produce.

In an ideal scenario, rapid and cost-effective biosensors with high accuracy would facilitate high spatiotemporal resolution to identify: i) presence/absence of target pathogen(s), ii) concentration of target pathogen species, and iii) whether the contamination is transient contamination or persistent contamination. Some biosensors to date are capable of achieving the first aim (presence/absence) at relatively low concentrations (e.g., LOD of approximately 10 CFU/mL for many food-related bacterial pathogens [92]) but suffer from poor selectivity for complex samples (including biofilms).

According to the World Health Organization global strategy for food safety [107], there is an urgent need to strengthen testing and monitoring capacity in the food system, particularly in developing countries [108–110]. Biosensors coupled with decision support systems are an emerging tool for early warning and can provide risk reduction and improved management of key aspects in the food supply chain [111]. SDG3 states the need to ensure good health and well-being for all. One of the global threats to human health is foodborne pathogens such as *L. monocytogenes* [112, 113]. The main impacts of FBD outbreaks include major economic loss, food waste, hospitalizations and deaths from the infection. FBD disproportionately affects developing countries, such as the outbreak that occurred in South Africa between 2017 and 2018 that resulting in 204 deaths [25]. Improved food safety monitoring and decision support systems are a key technology innovation that can make major contributions to the ONE health paradigm [114].

## 4 Conclusions

In this manuscript, aptasensors were developed based on a metallized laser-inscribed graphene (LIG) electrode platform. This is the first demonstration of a *L. monocytogenes* biosensor on LIG, which paves the way forward for development of low-cost, scalable biosensors using recently established manufacturing approaches. After exploring multiple DNA aptamers from the literature and performing preliminary screening analysis, a binary mixed aptamer biosensor design was demonstrated, which is a new concept in whole cell bacteria aptasensors. Using this dual-aptamer strategy, an aptasensor was developed for targeting *L. monocytogenes* in lettuce hydroponic water. The multi-aptamer biosensor showed enhanced sensitivity, high accuracy (86%), lower LOD, and improved selectivity over other impedimetric biosensors in the current literature. Rapid screening of pathogens in agricultural water (including hydroponic water or other soil-less systems) for fresh produce is a global need to meet food safety and water quality safety needs.

**Acknowledgements** This project was supported by Agriculture and Food Research Initiative Competitive Grant no. 2018-67016-27578 awarded as a Center of Excellence from the USDA National Institute of Food and Agriculture and also Grant no. 2023-38821-39796. The authors also acknowledge support from the National Science Foundation Nanobiosensors program (CBET- 1511953, CBET-1512659, and CBET- 1805512), as well as the Office of International Science and Engineering (PIRE-2230696). The authors thank Dr. Jones at University of Florida for use of Hygeina PCR system and we gratefully acknowledge technical support teams at GeneLink and Nicoya Life Sciences for troubleshooting assistance. We also thank Dr. Pat Millner at USDA-ARS-NEA-BARC for assistance with design of microbiological testing. A pre-print/part of this work can be found in the MIT DSpace library at: https://dspace.mit.edu/handle/1721.1/123983 .

**Author contributions** Conceptualization: N.C., E.S.M.; Data Curation: E.S.M., S.P.A.D.; Formal Analysis/Visualization: N.C., G.M., D.V., E.S.M.; Funding Acquisition: D.V., E.S.M.; C.G.; Investigation/Methodology: N.C., E.S.M.; Resources: C.G., S.P.A.D., E.S.M.; Writing: N.C., G.M, D.V., D.X., S.P.A.D., C.G., E.S.M.

**Data availability** The raw electrochemical sensing data have been deposited in the Zenodo community "SmartPath Sensors", and are available as csv files at the following open access data repository: https://zenodo.org/communities/smartpathsensors. https://doi.org/10.5281/zenodo.10719208

## Declarations

**Competing interests** The authors declare no competing interests.



## References

1. Hebinck A, et al. Exploring the transformative potential of urban food. npj Urban Sustain. 2021;1:38.
2. McPhearson T, et al. Radical changes are needed for transformations to a good Anthropocene. npj Urban Sustain. 2021;1:5.
3. Lefers RM, Tester M, Lauersen KJ. Emerging technologies to enable sustainable controlled environment agriculture in the extreme environments of middle East-North Africa coastal regions. Front Plant Sci. 2020. https://doi.org/10.3389/fpls.2020.00801.
4. Dsouza A, Newman L, Graham T, Fraser EDG. Exploring the landscape of controlled environment agriculture research: a systematic scoping review of trends and topics. Agric Syst. 2023;209: 103673.
5. Walters KJ, Behe BK, Currey CJ, Lopez RG. Historical, current, and future perspectives for controlled environment hydroponic food crop production in the United States. HortScience. 2020;55:758–67.
6. Erekath S, Seidlitz H, Schreiner M, Dreyer C. Food for future: exploring cutting-edge technology and practices in vertical farm. Sustain Cities Soc. 2024;106: 105357.
7. Cifuentes-Torres L, Mendoza-Espinosa LG, Correa-Reyes G, Daesslé LW. Hydroponics with wastewater: a review of trends and opportunities. Water Environ J. 2021;35:166–80.
8. Sucozhañay A, et al. Rainwater harvesting as a sustainable solution for the production of urban hydroponic crops. Water Reuse. 2024;14:177–89.
9. Jurga A, Pacak A, Pandelidis D, Kaźmierczak B. A long-term analysis of the possibility of water recovery for hydroponic lettuce irrigation in an indoor vertical farm part 2: rainwater harvesting. Appl Sci. 2020;11:310.
10. Coon D, et al. Reporting and practices of sustainability in controlled environment agriculture: a scoping review. Environ Syst Decis. 2024;44:301–26.
11. Pérez-Escamilla R. Food security and the 2015–2030 sustainable development goals: from human to planetary health. Curr Dev Nutr. 2017;1: e000513.
12. Havelaar AH, et al. World health organization global estimates and regional comparisons of the burden of foodborne disease in 2010. PLoS Med. 2015;12: e1001923.
13. Pires SM, et al. Burden of foodborne diseases: think global, act local. Curr Opin Food Sci. 2021;39:152–9.
14. Shamloo E, et al. Importance of Listeria monocytogenes in food safety: a review of its prevalence, detection, and antibiotic resistance. Iran J Vet Res. 2019;20:241–54.
15. Hoffmann, S. Cost estimates of foodborne illnesses. *USDA Economic Research Service*. https://www.ers.usda.gov/data-products/cost-estimates-of-foodborne-illnesses.aspx (2022).
16. Heo EJ, Kim H-Y, Suh SH, Moon JS. Comparison of DNA extraction methods for the quantification of listeria monocytogenes in dairy products by real-time quantitative PCR&gt. J Food Prot. 2022;85:1531–7.
17. Zhang X, Wang S, Chen X, Qu C. Review controlling Listeria monocytogenes in ready-to-eat meat and poultry products: an overview of outbreaks, current legislations, challenges, and future prospects. Trends Food Sci Technol. 2021;116:24–35.
18. Phan TN, Miyamoto T, Masuda Y, Hohjoh K, Thi ANT. Occurrence, antimicrobial resistance, and genetic diversity of Listeria monocytogenes at fish-processing plants in Vietnam. Food Sci Technol Res. 2022;28:141.
19. Townsend A, Strawn LK, Chapman BJ, Dunn LL. A systematic review of listeria species and listeria monocytogenes prevalence, persistence, and diversity throughout the fresh produce supply Chain. Foods. 2021;10:1427.
20. Townsend A, et al. Factors that predict Listeria prevalence in distribution centers handling fresh produce. Food Microbiol. 2022;107: 104065.
21. Charpentier E, Courvalin P. Antibiotic resistance in *Listeria* spp. Antimicrob Agents Chemother. 1999;43:2103–8.
22. Sibanda T, Buys EM. Listeria monocytogenes pathogenesis: the role of stress adaptation. Microorganisms. 2022;10:1522.
23. Barbuddhe SB, Chakraborty T. Listeria as an enteroinvasive gastrointestinal pathogen. Springer, Berlin Heidelberg: Berlin, Heidelberg; 2009.
24. Thomas J, et al. Outbreak of Listeriosis in South Africa associated with processed meat. N Engl J Med. 2020;382:632–43.
25. Olanya OM, et al. Cost estimation of listeriosis (Listeria monocytogenes) occurrence in South Africa in 2017 and its food safety implications. Food Control. 2019;102:231–9.
26. Ilic S, Moodispaw MR, Madden LV, Lewis Ivey ML. Lettuce contamination and survival of salmonella typhimurium and listeria monocytogenes in hydroponic nutrient film technique systems. Foods. 2022;11:3508.
27. Turner ER, Luo Y, Buchanan RL. Microgreen nutrition, food safety, and shelf life: a review. J Food Sci. 2020;85:870–82.
28. Kyere EO, et al. Biofilm formation of Listeria monocytogenes in hydroponic and soil grown lettuce leaf extracts on stainless steel coupons. LWT. 2020;126: 109114.

29. Estrada EM, et al. Prevalence, persistence, and diversity of listeria monocytogenes and listeria species in produce packinghouses in Three U.S. States. J Food Prot. 2020;83:277–86.
30. Dhulappanavar GR, Gibson KE. Persistence of Salmonella enterica subsp enterica ser Javiana, Listeria monocytogenes, and Listeria innocua in Hydroponic Nutrient Solution. J Food Prot. 2023;86: 100154.
31. Misra G, Gibson KE. Survival of Salmonella enterica subsp. enterica serovar Javiana and Listeria monocytogenes is dependent on type of soil-free microgreen cultivation matrix. J Appl Microbiol. 2020;129:1720–32.
32. Miceli A, Settanni L. Influence of agronomic practices and pre-harvest conditions on the attachment and development of Listeria monocytogenes in vegetables. Ann Microbiol. 2019;69:185–99.
33. Poltronieri P, Mezzolla V, Primiceri E, Maruccio G. Biosensors for the detection of food pathogens. Foods. 2014;3:511–26.
34. Wang S, Adekunle A, Raghavan V. Exploring the integration of bioelectrochemical systems and hydroponics: Possibilities, challenges, and innovations. J Clean Prod. 2022;366: 132855.
35. Kerry RG, Gouda S, Das G, Vishnuprasad CN, Patra JK. Agricultural nanotechnologies: current applications and future prospects. Microbial Biotechnol. 2017. https://doi.org/10.1007/978-981-10-6847-8_1.
36. Ragaveena S, Shirly Edward A, Surendran U. Smart controlled environment agriculture methods: a holistic review. Rev Environ Sci Biotechnol. 2021;20:887–913.
37. Lakicevic B, Jankovic V, Pietzka A, Ruppitsch W. Wholegenome sequencing as the gold standard approach for control of Listeria monocytogenes in the food chain. J Food Prot. 2023;86: 100003.
38. Lakicevic B, Nastasijevic I, Dimitrijevic M. Whole genome sequencing: an efficient approach to ensuring food safety. IOP Conf Ser Earth Environ Sci. 2017;85: 012052.
39. Välimaa A-L, Tilsala-Timisjärvi A, Virtanen E. Rapid detection and identification methods for Listeria monocytogenes in the food chain—a review. Food Control. 2015;55:103–14.
40. Sidhu RK, et al. Planar interdigitated aptasensor for flow-through detection of listeria spp In hydroponic lettuce growth media. Sensors. 2020;20:1–20.
41. Oliveira DA, Althawab S, McLamore ES, Gomes CL. One-step fabrication of stimuli-responsive chitosan-platinum brushes for listeria monocytogenes detection. Biosensors. 2021;11:511.
42. Vanegas DCDC, et al. Emerging biorecognition and transduction schemes for rapid detection of pathogenic bacteria in food. Compr Rev Food Sci Food Saf in press. 2017;1:18.
43. Hills KD, Oliveira DA, Cavallaro ND, Gomes CL, McLamore ES. Actuation of chitosan-aptamer nanobrush borders for pathogen sensing. Analyst. 2018;143:1650–61.
44. Soni DK, Ahmad R, Dubey SK. Biosensor for the detection of Listeria monocytogenes: emerging trends. Crit Rev Microbiol. 2018;44:590–608.
45. Gupta P, Adhikari A. Novel approaches to environmental monitoring and control of listeria monocytogenes in food production facilities. 2022. Foods. https://doi.org/10.3390/foods11121760.
46. Tang Y, Moreira GA, Vanegas D, Datta SPA, McLamore ES. Batch-to-batch variation in laser-inscribed graphene (LIG) electrodes for electrochemical sensing. Micromachines. 2024;15:874.
47. Qian H, et al. Improving high throughput manufacture of laser-inscribed graphene electrodes via hierarchical clustering. Sci Rep. 2024;14:7980.
48. Tan PS, et al. Laser scribing fabrication of graphitic carbon biosensors for label-free detection of interleukin-6. Nanomaterials. 2021;11:2110.
49. Wagh MD, Sahoo SK, Goel S. Laser-induced graphene ablated polymeric microfluidic device with interdigital electrodes for taste sensing application. Sens Actuators A Phys. 2022;333: 113301.
50. Kucherenko IS, et al. Laser-induced graphene electrodes for electrochemical ion sensing, pesticide monitoring, and water splitting. Anal Bioanal Chem. 2021;413:6201–12.
51. Vanegas D, et al. Laser scribed graphene biosensor for detection of biogenic amines in food samples using locally sourced materials. Biosensors. 2018;8:42.
52. Yagati AK, et al. Laser-induced graphene interdigitated electrodes for label-free or nanolabel-enhanced highly sensitive capacitive aptamer-based biosensors. Biosens Bioelectron. 2020;164: 112272.
53. Amouzadeh Tabrizi M, Acedo P. Highly sensitive aptasensor for the detection of SARS-CoV-2-RBD using aptamer-gated methylene blue@ mesoporous silica film/laser engraved graphene electrode. Biosens Bioelectron. 2022;215: 114556.
54. Pola CC, et al. Aerosol-jet-printed graphene electrochemical immunosensors for rapid and label-free detection of SARS-CoV-2 in saliva. Materials. 2022;9: 035016.
55. Gerstl F, Pongkitdachoti U, Unob F, Baeumner AJ. Miniaturized sensor for electroanalytical and electrochemiluminescent detection of pathogens enabled through laser-induced graphene electrodes embedded in microfluidic channels. Lab Chip. 2022;22:3721–33.
56. Moreira G, et al. Development of a biosensor based on angiotensin-converting enzyme II for severe acute respiratory syndrome coronavirus 2 detection in human saliva. Front Sens. 2022;3: 917380.
57. Soares RRA, et al. Laser-induced graphene electrochemical immunosensors for rapid and label-free monitoring of salmonella enterica in chicken broth. ACS Sens. 2020;5:1900–11.
58. Fenzl C, et al. Laser-scribed graphene electrodes for aptamer-based biosensing. ACS Sens. 2017;2:616–20.
59. Moreira G, et al. A capacitive laser-induced graphene based aptasensor for SARS-CoV-2 detection in human saliva. PLoS ONE. 2023;18: e0290256.
60. Ohk SH, Koo OK, Sen T, Yamamoto CM, Bhunia AK. Antibody-aptamer functionalized fibre-optic biosensor for specific detection of Listeria monocytogenes from food. J Appl Microbiol. 2010;109:808–17.
61. Lee S-H, et al. Analytical bioconjugates, aptamers, enable specific quantitative detection of Listeria monocytogenes. Biosens Bioelectron. 2015;68:272–80.
62. Burrs SL, et al. A paper based graphene-nanocauliflower hybrid composite for point of care biosensing. Biosens Bioelectron. 2016;85:479–87.

63. Giacobassi CA, et al. Sense–Analyze–respond–actuate (SARA) paradigm: proof of concept system spanning nanoscale and macroscale actuation for detection of escherichia coli in aqueous media. Actuators. 2020;10:2.
64. Castillo-Torres KY, Arnold DP, McLamore ES. Rapid isolation of Escherichia coli from water samples using magnetic microdiscs. Sens Actuators B Chem. 2019. https://doi.org/10.1016/j.snb.2019.04.043.
65. Castillo-Torres KY, McLamore ES, Arnold DP. A high-throughput microfluidic magnetic separation (μFMS) platform for water quality monitoring. Micromachines. 2020. https://doi.org/10.3390/mi11010016.
66. Qian H, McLamore E, Bliznyuk N. Machine learning for improved detection of pathogenic *E coli* in hydroponic irrigation water using impedimetric aptasensors: a comparative study. ACS Omega. 2023;8:34171–9.
67. Oliveira DA, McLamore ES, Gomes CL. Rapid and label-free Listeria monocytogenes detection based on stimuli-responsive alginate-platinum thiomer nanobrushes. Sci Rep. 2022;12:21413.
68. GeneLink. *Thiol Modified Oligo Disulfide Reduction*. (2023).
69. McLamore ES, Vanegas DC, Pinzon DB, McCourt K, Tang Y. Protocol L23-LIG fabrication using Universal Laser System. Protcol. 2020. https://doi.org/10.17504/protocols.io.byc4psyw.
70. McLamore ES, Vanegas DC, Pinzon DB, McCourt K, Tang Y. Protocol L2.3-LIG fabrication using Universal Laser System. Protcol. 2020. https://doi.org/10.17504/protocols.io.byc4psyw.
71. Taguchi M, et al. pulSED: pulsed sonoelectrodeposition of fractal nanoplatinum for enhancing amperometric biosensor performance. Analyst. 2016;141:3367–78.
72. Shi J, et al. Oscillatory glucose flux in INS 1 pancreatic β cells: a self-referencing microbiosensor study. Anal Biochem. 2011. https://doi.org/10.1016/j.ab.2010.12.019.
73. Garland NT, et al. Flexible laser-induced graphene for nitrogen sensing in soil. ACS Appl Mater Interfaces. 2018. https://doi.org/10.1021/acsami.8b10991.
74. Hjort RG, et al. Hydrophobic laser-induced graphene potentiometric ion-selective electrodes for nitrate sensing. Microchim Acta. 2022;189:122.
75. Tang Y, et al. Electrochemical analysis of laser-inscribed graphene electrodes using cyclic voltammetry (ferri/ferrocyanide redox couple). Protcol. 2023;1:13.
76. Li K, et al. An ultrafast conducting Polymer@MXene positive electrode with high volumetric capacitance for advanced asymmetric supercapacitors. Small. 2020;16:1906851.
77. Jenkins DM, Lee BE, Jun S, Reyes-De-Corcuera J, McLamore ES. ABE-Stat, a fully open-source and versatile wireless potentiostat project including electrochemical impedance spectroscopy. J Electrochem Soc. 2019. https://doi.org/10.1149/2.0061909jes.
78. Thomsen V, Schatzlein D, Mercuro D. Limits of detection in spectroscopy. Spectroscopy. 2003;18:112–4.
79. Ruopp MD, Perkins NJ, Whitcomb BW, Schisterman EF. Youden index and optimal cut-point estimated from observations affected by a lower limit of detection. Biom J. 2008;50:419–30.
80. Shan G. Improved confidence intervals for the youden index. PLoS ONE. 2015;10: e0127272.
81. Felder S, Mayrhofer T. Medical decision making. Springer, Berlin Heidelberg: Berlin, Heidelberg; 2017.
82. Puetz P, Behrent A, Baeumner AJ, Wegener J. Laser-scribed graphene (LSG) as new electrode material for impedance-based cellular assays. Sens Actuators B Chem. 2020;321: 128443.
83. Behrent A, Griesche C, Sippel P, Baeumner AJ. Process-property correlations in laser-induced graphene electrodes for electrochemical sensing. Microchim Acta. 2021;188:1–14.
84. Ullah SF, Moreira G, Datta SPA, McLamore E, Vanegas D. An experimental framework for developing point-of-need biosensors: connecting bio-layer interferometry and electrochemical impedance spectroscopy. Biosensors. 2022;12:938.
85. Qureshi A, Roci I, Gurbuz Y, Niazi JH. An aptamer based competition assay for protein detection using CNT activated gold-interdigitated capacitor arrays. Biosens Bioelectron. 2012;34:165–70.
86. Berggren C, Bjarnason B, Johansson G. Capacitive biosensors. Electroanalysis. 2001;13:173–80.
87. Cabanes D, Dehoux P, Dussurget O, Frangeul L, Cossart P. Surface proteins and the pathogenic potential of Listeria monocytogenes. Trends Microbiol. 2002;10:238–45.
88. Bierne H, Cossart P. *Listeria monocytogenes* surface proteins: from genome predictions to function. Microbiol Mol Biol Rev. 2007;71:377–97.
89. Liu Y, Yu H, Alkhamis O, Moliver J, Xiao Y. Tuning biosensor cross-reactivity using aptamer mixtures. Anal Chem. 2020;92:5041–7.
90. Drabovich AP, Okhonin V, Berezovski M, Krylov SN. Smart aptamers facilitate multi-probe affinity analysis of proteins with ultra-wide dynamic range of measured concentrations. J Am Chem Soc. 2007;129:7260–1.
91. Pan J, et al. Electrochemical aptamer-based sensors with Tunable detection range. Anal Chem. 2023;95:420–32.
92. Vanegas DC, Gomes CL, Cavallaro ND, Giraldo-Escobar D, McLamore ES. Emerging biorecognition and transduction schemes for rapid detection of pathogenic bacteria in food. Compr Rev Food Sci Food Saf. 2017;16:1188–205.
93. Tambi A, Brighu U, Gupta AB. Methods for detection and enumeration of coliforms in drinking water: a review. Water Supply. 2023;23:4047–58.
94. Hijnen WAM, Suylen GMH, Bahlman JA, Brouwer-Hanzens A, Medema GJ. GAC adsorption filters as barriers for viruses, bacteria and protozoan (oo)cysts in water treatment. Water Res. 2010;44:1224–34.
95. Hijnen W, et al. Enumeration of faecal indicator bacteria in large water volumes using on site membrane filtration to assess water treatment efficiency. Water Res. 2000;34:1659–65.
96. Radhakrishnan R, Jahne M, Rogers S, Suni II. Detection of listeria monocytogenes by electrochemical impedance spectroscopy. Electroanalysis. 2013;25:2231–7.
97. Chemburu S, Wilkins E, Abdel-Hamid I. Detection of pathogenic bacteria in food samples using highly-dispersed carbon particles. Biosens Bioelectron. 2005;21:491–9.
98. Ding J, Lei J, Ma X, Gong J, Qin W. Potentiometric aptasensing of Listeria monocytogenes using protamine as an indicator. Anal Chem. 2014;86:9412–6.
99. Wang D, et al. Efficient separation and quantitative detection of Listeria monocytogenes based on screen-printed interdigitated electrode, urease and magnetic nanoparticles. Food Control. 2017;73:555–61.

100. Kanayeva DA, et al. Efficient separation and sensitive detection of listeria monocytogenes using an impedance immunosensor based on magnetic nanoparticles, a microfluidic chip, and an interdigitated microelectrode. J Food Prot. 2012;75:1951–9.
101. Sheng L, Zhu M-J. Practical in-storage interventions to control foodborne pathogens on fresh produce. Compr Rev Food Sci Food Saf. 2021;20:4584–611.
102. Soon JM, Brazier AKM, Wallace CA. Determining common contributory factors in food safety incidents—a review of global outbreaks and recalls 2008–2018. Trends Food Sci Technol. 2020;97:76–87.
103. Zwirzitz B, et al. Co-occurrence of listeria spp and spoilage associated microbiota during meat processing due to cross-contamination events. Front Microbiol. 2021. https://doi.org/10.3389/fmicb.2021.632935.
104. Zoellner C, Ceres K, Ghezzi-Kopel K, Wiedmann M, Ivanek R. Design elements of listeria environmental monitoring programs in food processing facilities: a scoping review of research and guidance materials. Compr Rev Food Sci Food Saf. 2018;17:1156–71.
105. Powell MR. Optimal food safety sampling under a budget constraint. Risk Anal. 2014;34:93–100.
106. Magdovitz BF, et al. Analyzing aggregate environmental monitoring data for Listeria spp. in frozen food manufacturing environments. Food Control. 2022;135:108746.
107. WHO NFS (Nutrition and Food Safety). WHO Global Strategy for Food Safety 2022–2030: Towards Stronger Food Safety Systems and Global Cooperation. Geneva: World Health Organization; 2022.
108. Morse T, Masuku H, Rippon S, Kubwalo H. Achieving an integrated approach to food safety and hygiene—meeting the sustainable development goals in Sub-Saharan Africa. Sustainability. 2018;10:2394.
109. Flynn K, et al. An introduction to current food safety needs. Trends Food Sci Technol. 2019;84:1–3.
110. Unnevehr LJ. Addressing food safety challenges in rapidly developing food systems. Agric Econ. 2022;53:529–39.
111. McLamore ES, Datta SPA. A connected world: system-level support through biosensors. Annu Rev Anal Chem. 2023;16:285–309.
112. Hamon M, Bierne H, Cossart P. Listeria monocytogenes: a multifaceted model. Nat Rev Microbiol. 2006;4:423–34.
113. Buchanan RL, Gorris LGM, Hayman MM, Jackson TC, Whiting RC. A review of Listeria monocytogenes : an update on outbreaks, virulence, dose-response, ecology, and risk assessments. Food Control. 2017;75:1–13.
114. Garcia SN, Osburn BI, Jay-Russell MT. One health for food safety, food security, and sustainable food production. Front Sustain Food Syst. 2020. https://doi.org/10.3389/fsufs.2020.00001.